Disjoint and coextensive diradical diions

Richard J. Bushby, David R. McGill, Kai M. Ng and Norman Taylor

School of Chemistry, The University Of Leeds, Leeds, UK LS2 9JT

***N*,*N*,*N′*,*N′*-Tetraanisyl-3,3′-diaminobiphenyl and *N*,*N*,*N′*,*N′*-tetraanisyl-3,4′-diaminobiphenyl have been synthesised and their oxidations studied by cyclic voltammetry and EPR spectroscopy. A two-electron oxidation of the former species gives a π system which is disjoint and oxidation of the latter gives a π system which is coextensive. Cyclic voltammetry is shown to be a useful tool for revealing the difference between the disjoint and coextensive π systems. The coulombic contribution to the difference between the half-wave potentials for the first and second oxidation steps (ΔE), which measures the 'hole–hole' repulsion energy, was extracted by measuring ΔE as a function of the relative permittivity of the medium. This was substantially greater in the coextensive case. Both diradical diions gave triplet EPR spectra. A comparison of the cyclic voltammetry of *N*,*N*,*N′*,*N′*-tetraanisyl-3,4′-diaminobiphenyl and that of a high-spin polymer precursor with the same local topology showed that, in the oxidised polymer, the additional hole–hole repulsion energy associated with the coextensive spin–spin distribution is of the order of 0.1–0.2 V—a noticeable effect but not one large enough to explain the difficulties that have been encountered in achieving high doping levels in this and related high-spin polymers.**

This paper shows that cyclic voltammetry can be used as a tool to reveal the basic difference between disjoint and coextensive diradical diion systems and that the additional charge–charge repulsion energy intrinsic in coextensive radical ions is measurable but that it is not sufficient to explain the difficulties experienced in producing high-spin polymers based on a local coextensive radical ion topology.

The disjoint–coextensive division is fundamental to diradical chemistry.[1,2] Only coextensive diradicals exhibit those strong exchange interactions which stabilise the triplet over the singlet state. In Fig. 1 the situation is illustrated for an isomeric pair of π-diradicals in the non-Kekulé quinodimethane series[3] but the analysis applies equally well to any other class of diradical.[3] The 3,3′-dimethylene system **1** is disjoint. The degenerate singly occupied orbitals Ψ_7 and Ψ_8 are spatially distinct [Fig. 1(*b*), (*c*)]. There is no direct communication between the spins and the singlet and triplet states are expected to be almost degenerate. On the other hand the 3,4′-dimethylene system **2** is coextensive. The degenerate singly occupied orbitals Ψ_7 and Ψ_8 are orthogonal but they overlap in their spatial distributions. There will be a strong exchange interaction and the triplet state will be strongly favoured. This is the molecular–molecular orbital equivalent of Hund's rule as it is normally applied to atomic–atomic orbital systems.[1] Degenerate, singly occupied orbitals with coextensive spin distributions are associated with a large exchange interaction and a high-spin ground state. Experimental confirmation of the correctness of this analysis is provided by the observation that the carbene **3** and the nitrene **5** have singlet ground states and the carbene **4** and the nitrene **6** have pentuplet ground states.[4,5] (The analysis of preferred spin states for carbenes and nitrenes follows that for the diradicals **1** and **2** since the coupling of the spins between the two carbene–nitrene centres is mediated through the π electron components).

As a first-order approximation, when a closed-shell molecule undergoes a one-electron oxidation, the spin and 'hole' (change in charge) distributions in the resultant radical cation are the same. Similarly, and again to a first-order approximation, a two-electron oxidation of a molecule containing two otherwise equal sites, will produce a diradical dication in which the spin–spin and hole–hole interactions relate to each other. Hence, in the production of equivalent disjoint and coextensive diradical dications, we expect to see an additional hole–hole repulsion in

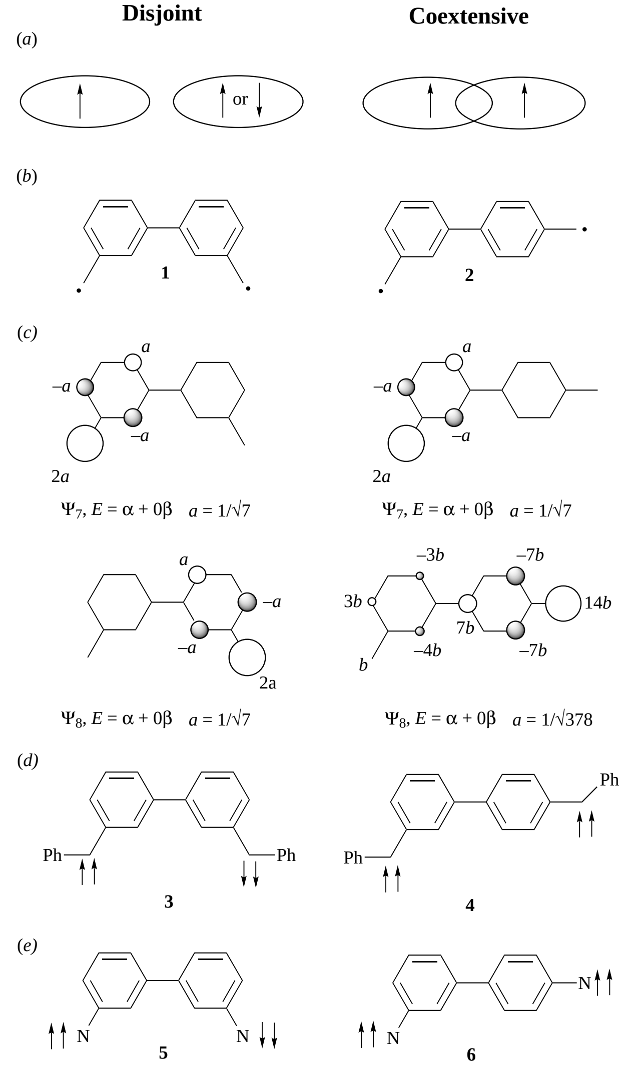

Fig. 1 (*a*) Schematic representation of the spin distributions of the unpaired electrons in disjoint and coextensive diradicals; (*b*) 3,3′-dimethylenebiphenyl and 3,4′-dimethylenebiphenyl; (*c*) spatial distributions for the singly occupied non-bonding molecular orbitals; (*d*) and (*e*) equivalent carbene and nitrene systems

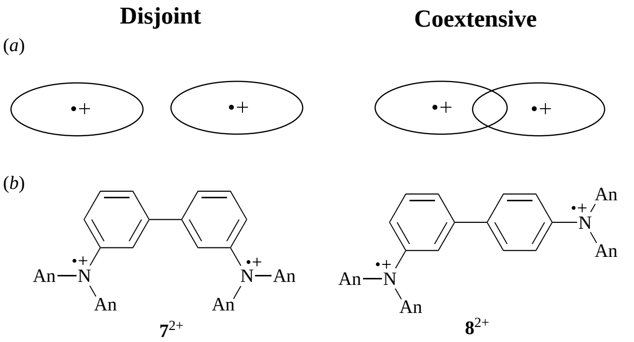

Fig. 2 (*a*) Schematic representation of the charge and spin distributions in disjoint and coextensive diradical diions; (*b*) *N*,*N*,*N*′,*N*′-tetraanisyl-3,3′-diaminobiphenyl and *N*,*N*,*N*′,*N*′-tetraanisyl-3,4′-diaminobiphenyl diradical dications

the coextensive case related to its coextensive nature. It should be possible to measure this as it is the coulombic part of the difference between the half-wave potentials for the first and second oxidation steps—that part that is inversely proportional to the relative permittivity of the medium. This expectation is confirmed by the present study of the oxidation of the diamines **7** and **8**. The diradical dications $\mathbf{7}^{2+}$ and $\mathbf{8}^{2+}$ (Fig. 2) obtained by two-electron oxidations of these amines are isoelectronic with their quinodimethane counterparts. The dication $\mathbf{7}^{2+}$ belongs to the disjoint category and the dication $\mathbf{8}^{2+}$ to the coextensive category. There were two main reasons for choosing these aza derivatives. First, the radical cations are relatively stable. Most quinodimethanes are only stable at low temperatures in frozen matrices but the dications $\mathbf{7}^{2+}$ and $\mathbf{8}^{2+}$, like some other $Ar_3N^{\bullet+}$ radical cations, are stable in solution at room temperature. Secondly, we and others have become interested in using the polyradical polycations derived by oxidation of arylamine polymers and related oligomers in our attempts to construct organic molecular magnets.[6] In this context, it is proving important to understand their redox properties, in particular, the extent to which doping by either chemical or electrochemical methods is affected and perhaps even limited by repulsive coulombic interactions.

Results

Synthesis

Biphenyls which contain primary amino- or nitro-groups in the 4-position are notoriously potent carcinogens[7] but those with groupings only in the 3-positions are much less active. Hence, in the 3,3′-series a simple synthesis could be performed using the 3,3′-diamine **11** (Scheme 1) as the key intermediate. An Ullmann coupling of the commercially available *meta*-nitroiodobenzene **9** gave the biphenyl **10** which was reduced to the diamine **11** and converted to the tetraanisyl derivative **7** by reaction with 4-iodoanisole in the presence of copper and potassium carbonate.[8]

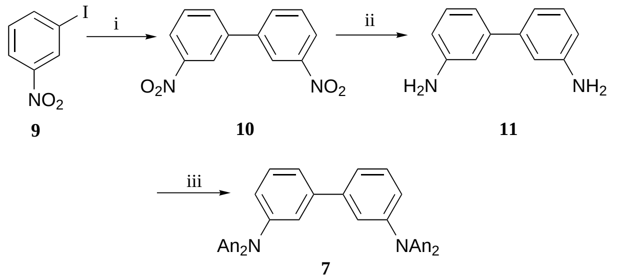

Scheme 1 Synthesis of the diamine **7**. *Reagents and conditions*: i Cu, DMF, reflux, 48%; ii Sn, conc. HCl, EtOH, 98%; iii 4-iodoanisole, Cu, K_2CO_3, *o*-dichlorobenzene, 64%. An = *p*-$MeOC_6H_4$.

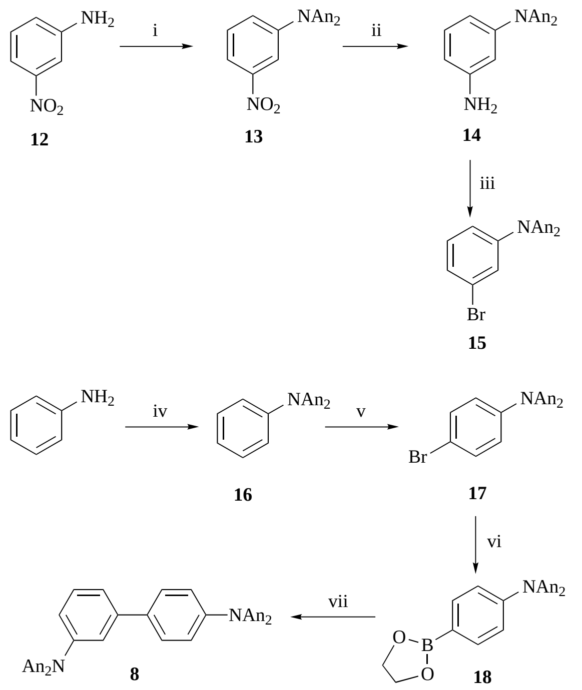

Scheme 2 Synthesis of the diamine **8**. *Reagents and conditions*: i 4-iodoanisole, Cu, K_2CO_3, DMF, reflux, 52%; ii H_2, Raney Ni, EtOH, 100%; iii HBr, $NaNO_2$, $Cu^{(I)}Br$, <0 °C, 43%; iv 4-iodoanisole, $Cu^{(I)}I$, K_2CO_3, *o*-dichlorobenzene, 83%; v Br_2, $CHCl_3$, 0 °C, 95%; vi (a) Bu^nLi, THF, −78 °C, Ar, (b) $(Pr^iO)_3B$, THF, −78 °C, Ar, (c) H^+, H_2O, (d) ethane-1,2-diol, 100 °C/0.1 mmHg, 65%; vii compound **15**, $Pd(PPh_3)_4$, $Ba(OH)_2$, toluene, reflux, 75%.

In the 3,4′-disubstituted series an indirect route was chosen to avoid making the 3,4′-diamine (Scheme 2). The key step is the Suzuki coupling[9] of the two tertiary amino compounds **15** and **18**. The *meta*-bromo compound **15** was prepared from *meta*-nitroaniline **12** by reaction with 4-iodoanisole, reduction of the nitro group and its conversion to a bromo substituent through a Sandmeyer reaction. The intermediate diamino compound **14** proved highly susceptible to aerial oxidation. The boronic acid derivative **18** was prepared from aniline by reaction with 4-iodoanisole, bromination of the free *para*-position and conversion of the bromo to the 1,3,2-dioxaborolane derivative in the usual manner. This derivative was chosen because of difficulties in characterising the equivalent boronic acid.[10]

Using these synthetic routes both of the desired substrates **7** and **8** could be made pure on a gram scale.

Electrochemical studies

The splitting ΔE between the half-wave potentials for the first and second oxidation steps for the diamines **7** and **8** was studied as a function of solvent polarity and supporting electrolyte concentration in benzonitrile, chloroform, benzonitrile–chloroform mixtures and dichloromethane using tetrabutylammonium hexafluorophosphate as the supporting electrolyte. These particular solvent mixtures encompass a wide range of bulk relative permittivities. More conventional mixed solvents based on acetonitrile, dimethyl sulfoxide, dimethylformamide, *etc.* as the polar component gave problems either because the redox steps proved to be irreversible or because the compounds were insufficiently soluble. Fig. 3 shows cyclic voltammetry results and those obtained by convolution–deconvolution methods *via* dI_1/dE (where I_1 is the semi-integral of the current i *vs.* time)[11] for both of the diamines. The latter method was chosen since, for fast electron transfer (reversible) systems, I_1 is a function of E only, irrespective of whether the potential changes at the electrodes are strictly linear or not. In the case of high resistance electrolytes, convolution criteria must supplant those applicable to linear sweep cyclic voltammograms and they

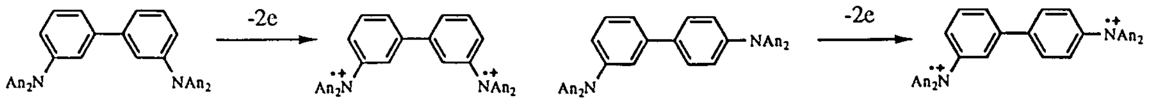

7 $\quad$ **7**$^{2+}$ $\quad$ **8** $\quad$ **8**$^{2+}$

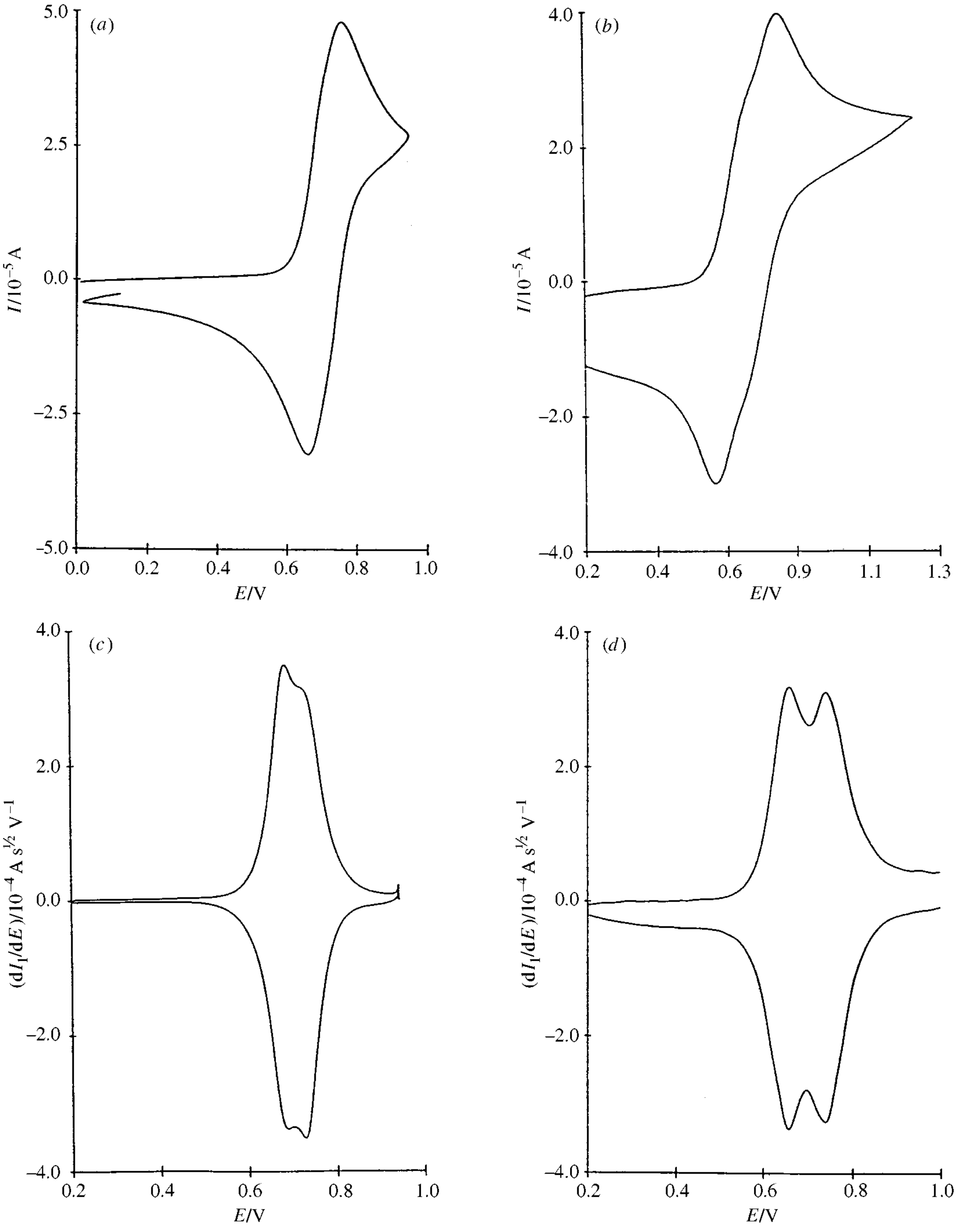

Fig. 3 (*a*) and (*b*) Typical cyclic voltammograms for 10^{-3} M *N,N,N′,N′*-tetraanisyl-3,3′-diaminobiphenyl **7** and *N,N,N′,N′*-tetraanisyl-3,4′-diaminobiphenyl **8** in dichloromethane with 0.1 M tetrabutylammonium hexafluorophosphate as the supporting electrolyte. The scale is referenced to silver/silver chloride. (*c*) and (*d*) The corresponding deconvolution plots.

have the added advantage of symmetry in the display. In the dI_1/dE plots the splitting between the first and second half-wave potentials is very clear as is the greater splitting in the case of compound **8**. The maxima in dI_1/dE *vs.* E only correspond to $E_{\frac{1}{2}}$ when there is 'baseline separation' of the peaks. When the splittings are small (as in this case) they cannot be measured directly from the maxima and so they were determined from the half-widths of the overall dI_1/dE response by direct comparison with the simulated values obtained using the CONDESIM software suite. Using this approach a reproducibility in the measured splittings of *ca.* 1 mV was achieved which was an order of magnitude better than the reproducibility in the absolute values of the half-wave potentials. The results are summarised in Tables 1–4.

Fig. 4 shows the dependence of the splittings for diamines **7** and **8** as a function of the bulk relative permittivity of the medium for mixtures of benzonitrile and chloroform. In all cases, the relative permittivity used, ε_u, was the weighted average of the bulk values for the two solvents and was uncorrected for the presence of the electrolyte (0.1 M in all systems).[12] The general form of the plots shown in Fig. 4 is very similar to those which we have previously reported for bimetallic complexes of

Table 1 Cyclic voltammetry results for *N*,*N*,*N*′,*N*′-tetraanisyl-3,3′-diaminobiphenyl **7** in benzonitrile–chloroform with 0.1 M tetrabutylammonium hexafluorophosphate as the supporting electrolyte and conductance (in the cell used) for 0.1 M tetrabutylammonium hexafluorophosphate in the same solvent mixtures. The oxidation potentials $E_1°$ and $E_2°$ are quoted relative to ferrocene/ferrocenium = 0 both separately measured for each solvent mixture used relative to silver/silver chloride.

Benzonitrile (%)	ε_u	$E_1°$/ mV	$E_2°$/ mV	ΔE/ mV	ΔE_{corr}/ mV	$G/10^{-3}\ \Omega^{-1}$
100	25.2	245	307	62	27	2.36
95	24.2	247	309	62	27	2.31
90	23.2	244	306	63	28	2.27
85	22.2	243	307	63	28	2.23
80	21.2	243	307	64	29	2.20
75	20.1	244	308	65	30	2.17
70	19.1	243	309	65	30	2.14
65	18.1	242	308	66	31	2.06
60	17.1	242	310	68	33	1.98
55	16.1	240	308	68	33	1.95
50	15.1	241	309	68	33	1.87
45	14.1	244	310	66	31	1.80
40	13.1	240	305	65	30	1.68
30	11.1	240	302	63	28	1.40
20	9	241	307	60	25	1.01
10	7	240	294	54	19	0.67
0	5	238	282	44	9	0.33

Table 2 Cyclic voltammetry results for *N*,*N*,*N*′,*N*′-tetraanisyl-3,4′-diaminobiphenyl **8** in benzonitrile–chloroform with 0.1 M tetrabutylammonium hexafluorophosphate as the supporting electrolyte. The oxidation potentials $E_1°$ and $E_2°$ are quoted relative to ferrocene/ferrocenium = 0 both separately measured for each solvent mixture used relative to silver/silver chloride.

Benzonitrile (%)	ε_u	$E_1°$/mV	$E_2°$/mV	ΔE/mV
100	25.2	241	307	66
95	24.2	252	320	68
90	23.2	257	327	71
85	22.2	252	326	74
80	21.2	256	334	77
75	20.1	242	322	80
70	19.1	247	333	85
65	18.1	244	332	88
60	17.1	228	320	92
55	16.1	226	320	95
50	15.1	238	330	92
45	14.1	242	332	91
40	13.1	241	329	88
30	11.1	243	327	83
20	9	263	339	75
10	7	250	311	61
0	5	251	299	48

the type *cis*,*cis*-$M(CO)_4(\mu\text{-dppe})_2M^1(CO)_4$ [where M and M^1 are Cr, Mo or W, and dppe is 1,2-bis(diphenylphosphino)ethane] in dimethylformamide–dichloromethane–hexane mixtures,[13] and it has a similar explanation. In the high dielectric region (above ε_u *ca.* 15) the splitting decreases with increasing relative permittivity (as the solvent increasingly shields the hole–hole repulsion) but below ε_u *ca.* 15 the trend is reversed. This is attributed to the onset of ion-pair formation. This general conclusion is supported by the observation of an apparent break in the conductance *vs.* relative permittivity plot at about the same point (Fig. 5). As expected for a simple 'charge-controlled' phenomenon,[12] above ε_u *ca.* 15, a plot of ΔE *vs.* $1/\varepsilon_u$ is essentially linear (Fig. 6). The intercepts obtained by linear extrapolation to $1/\varepsilon_u = 0$ give the non-coulombic parts of ΔE which, as expected, are small; in the case of compound **7**, 16 mV, and for compound **8**, 8 mV.

As can be seen from the data in Tables 3 and 4, the value of ΔE is also a function of electrolyte concentration but this dependence is fairly small in the 'free ion' regime above ε_u *ca.* 15. In the ion pair regime (below ε_u *ca.* 15) the value of ΔE increases with decreasing concentration of the electrolyte as the fraction of ion pairs is reduced.

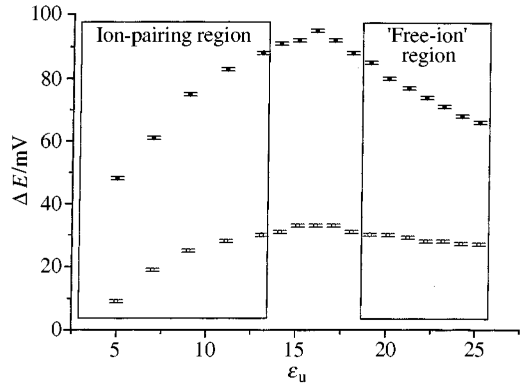

Fig. 4 The splitting ΔE between the first and second oxidation potentials of the diamines **7** and **8** plotted as a function of relative permittivity for mixtures of benzonitrile and chloroform. In all cases, the effective microscopic relative permittivity ε_u was taken as the weighted average of the bulk values for the two solvents and is uncorrected for the presence of the electrolyte (0.1 M tetrabutylammonium hexafluorophoshate).

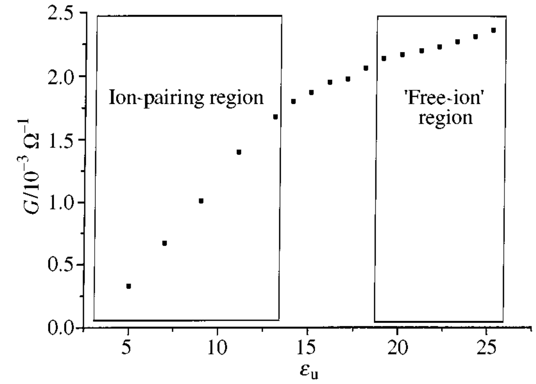

Fig. 5 Conductance of 0.1 M tetrabutylammonium hexafluorophosphate in mixtures of benzonitrile and chloroform plotted as a function of the relative permittivity

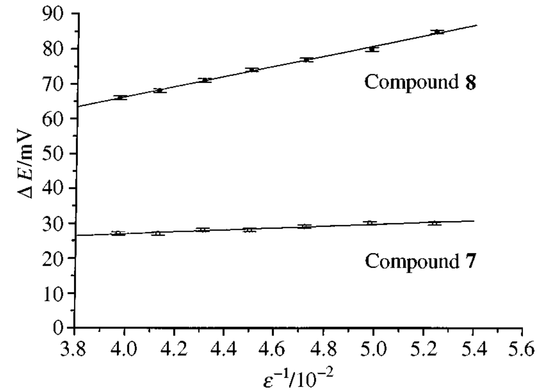

Fig. 6 The splitting ΔE between the first and second oxidation potentials of the diamines **7** and **8** plotted as a function of the inverse of the relative permittivity for mixtures of benzonitrile and chloroform in the 'free ion' regime

In the data given in Tables 1 and 3 the values of ΔE for the 3,3′-diamine have been corrected by subtracting an entropic factor of $(RT/nF)\ln 4$ (35 mV) to allow for the fact that the two oxidation sites here are chemically indistinguishable.[14]

It is interesting to note that the value of ε_u *ca.* 15 is close to the threshold value for ion-pairing noted in our previous study[13] and confirms that the transition region between 'free ion' and 'ion-pair' regimes is not particularly sensitive to the

Table 3 Cyclic voltammetry results for *N*,*N*,*N*′,*N*′-tetraanisyl-3,3′-diaminobiphenyl **7** in dichloromethane, benzonitrile, and chloroform at various concentrations of the supporting electrolyte (tetrabutylammonium hexafluorophosphate) and conductance for the supporting electrolyte

[TBAHFP]/M	ΔE_{corr}/ mV (CH_2Cl_2)	$G/10^{-3}\ \Omega^{-1}$ (CH_2Cl_2)	ΔE_{corr}/ mV (PhCN)	$G/10^{-3}\ \Omega^{-1}$ (PhCN)	ΔE_{corr}/ mV ($CHCl_3$)	$G/10^{-3}\ \Omega^{-1}$ ($CHCl_3$)
5E-1	—	2.60	25	4.90	—	1.60
2E-1	19	1.40	26	3.90	7	0.56
1E-1	22	0.65	28	2.50	9	0.33
5E-2	26	0.22	29	1.40	14	0.08
1E-2	31	0.09	30	0.55	21	0.008
5E-3	35	0.05	31	0.21	—	0.004
2E-3	34	0.03	32	0.08	—	0.001
1E-3	—	0.01	33	0.06	—	—

Table 4 Cyclic voltammetry results for *N*,*N*,*N*′,*N*′-tetraanisyl-3,4′-diaminobiphenyl **8** in dichloromethane and benzonitrile at various concentrations of the supporting electrolyte (tetrabutylammonium hexafluorophosphate)

[TBAHFP]/M	ΔE/mV (CH_2Cl_2)	ΔE/mV (PhCN)
5E-1	—	63
2E-1	62	65
1E-1	64	65
5E-2	68	67
1E-2	71	68
5E-3	76	69
2E-3	—	70
1E-3	—	72

exact chemical nature of the substrate or the solvent composition.

We are, however, principally interested in the region of high relative permittivity where it seems that the effects of ion-pairing can largely be ignored.

EPR studies

One-electron oxidation of the diamine **7** using trifluoroacetic acid–tetrabutylammonium tetrafluoroborate–dichloromethane at 260 K gave the spectrum for the monocation shown in Fig. 7(*a*). There is a splitting to a single nitrogen nucleus, *a*(1N) 9.5 G, together with many small hyperfine splittings, *a*(*n*H) *ca.* 0.5 G that could not be unambiguously assigned to specific hydrogens but which are doubtless attributable to hydrogens in the aromatic rings.[15] This splitting is most clearly resolved in the central component of the triplet.[16] A similar oxidation of the amine **8** using $NO^+BF_4^-$ in dichloromethane at 260 K gave the spectrum shown in Fig. 7(*b*) also showing a splitting to a single nitrogen nucleus, *a*(1N) 9.1 G, with many very small splittings due to the aromatic hydrogens, *a*(*n*H) *ca.* 0.5 G. Although the spectra shown in Fig. 7 were not obtained under exactly comparable conditions they do illustrate the fact that the monoradical from the diamine **7** generally showed more resolved fine structure. This may be because the spectrum from the amine **8** is actually an overlapping pair of slightly different spectra arising from two N-centred sites which, in terms of hyperfine structure, are inequivalent.

Two-electron oxidations of the diamines **7** and **8** to the dication level were carried out at room temperature using dichlorodicyanoquinone (DDQ)–trifluoroacetic acid in 2-methyltetrahydrofuran. Fig. 7(*c*) and (*d*) shows the resultant spectra for frozen glassy matrices at 100 K. These can both be interpreted as the summation of the powder spectra of one or two triplet species plus that of a doublet impurity. Simulations are shown in Fig. 7(*e*) and (*f*). The central line of each spectrum attributed to doublet impurities had essentially the same linewidth (*ca.* 10 G) as that obtained by oxidising trianisylamine under these conditions and freezing the resultant solution. Values of the zero field splittings $|D/hc|$ expected for the triplet dications $\mathbf{7}^{2+}$ and $\mathbf{8}^{2+}$ can be estimated on the basis of the hypothetical planar geometries, shown in Fig. 8.[18] Using standard bond lengths the nitrogen–nitrogen distances are 6.98 Å for the *cisoid* $\mathbf{7}^{2+}$, 8.43 Å for the *transoid* $\mathbf{7}^{2+}$ and 8.65 Å for $\mathbf{8}^{2+}$. Comparison with X-ray crystal structures for analogous triarylamines and triarylamine radical ions,[17] like molecular orbital and molecular mechanics calculations of the geometries of these compounds, shows that the aryl rings will not be coplanar. However, twisting of the nitrogen–aryl bonds does not affect the nitrogen–nitrogen distances so that the planar geometries provide a useful starting point. They lead to predicted values of $|D/hc| = 0.0051\ \mathrm{cm}^{-1}$ for the *cisoid* $\mathbf{7}^{2+}$, 0.0029 cm^{-1} for the *transoid* $\mathbf{7}^{2+}$. The simulation shown in Fig. 7(*e*) is based on two triplet species $|D/hc| = 0.0057\ \mathrm{cm}^{-1}$ and 0.0036 cm^{-1}. The predicted value of $|D/hc|$ for **8** is 0.0026 cm^{-1} which is in somewhat poorer agreement with the value of 0.0036 cm^{-1} used in the simulation shown in Fig. 7(*f*) but in either case the splittings are within normal error limits for these calculations.[3] No half-field lines were observed but nor would they be expected for triplets with such low zero-field splittings.[19] Attempts to measure the splitting of the singlet and triplet states by studying signal intensity as a function of temperature were frustrated by this absence of a $\Delta m = 2$ transition and by the strong dependence of the line shape of the $\Delta m = 1$ portion of the spectrum on temperature for compound **7** which made it impossible to reliably dissect out the contribution from the doublet component.[3,20] However, the lineshape for the EPR spectrum of the dication of **7** at 10 K was essentially that of the doublet component providing qualitative evidence that (as expected for a disjoint diradical diion) the triplet components of the spectra observed at 100 K are due to thermally populated states but that these are ground state singlet species. The simplest explanation of this unusual evolution of line shapes between 10 and 100 K is that the dependence of the thermal populations of the two components are different.

Discussion

The EPR spectra of the monoradical monocations $\mathbf{7}^+$ and $\mathbf{8}^+$ [Fig. 7(*a*) and (*b*)] only show a significant splitting to a single nitrogen nucleus and are essentially the same as those for any simple ring-substituted derivative of triphenylamine radical cation.[15] At the empirical level, this suggests that, perhaps, the corresponding diradical diions $\mathbf{7}^{2+}$ and $\mathbf{8}^{2+}$ should be thought of as an intramolecularly united but essentially independent pair of triphenylamine radical cations. Even if this were wholly true and there were no ‘leakage’ of charge or spin between the two halves of the molecule, the coulombic part of ΔE for the two amines **7** and **8** would show a small difference. The coulombic part of ΔE measures the *difference* in the field at the second triarylamine centre resulting from oxidation of the first and this will be different for the two diamines because the distances between the two centres are different. Using the hypothetical planar geometries, shown in Fig. 8, if it is assumed that the change in positive charge was all localised on the nitrogen or if it had a radially symmetric non-overlapping distribution about each nitrogen, the maximum difference in hole–hole

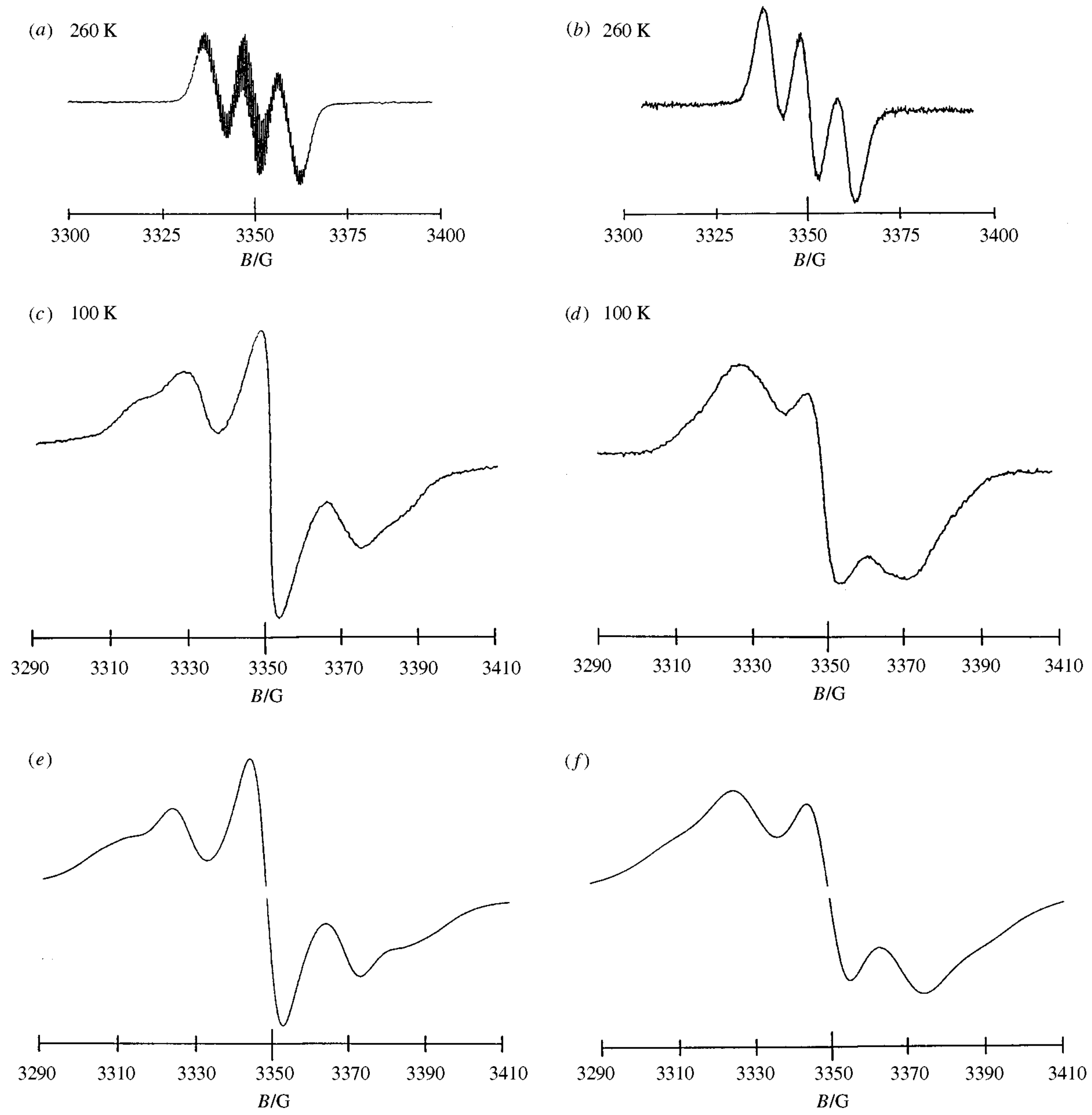

Fig. 7 EPR spectra for oxidation products of the diamines **7** and **8**. (*a*) $\mathbf{7}^{\bullet+}$, oxidation with trifluoroacetic acid–tetrabutylammonium tetrafluoroborate in dichloromethane at 260 K; (*b*) $\mathbf{8}^{\bullet+}$, oxidation with $NO^+BF_4^-$ in dichloromethane at 260 K; (*c*) $\mathbf{7}^{2+}$, frozen glassy matrix at 100 K, oxidation with dichlorodicyanoquinone and trifluoroacetic acid in 2-methyltetrahydrofuran; (*d*) $\mathbf{8}^{2+}$, frozen glassy matrix at 100 K, oxidation with dichlorodicyanoquinone and trifluoroacetic acid in 2-methyltetrahydrofuran; (*e*) simulation of the EPR spectrum shown above based on a 0.30 : 1.00 : 0.33 ratio of *cisoid* $\mathbf{7}^{2+}$, $|D/hc| = 0.0051\ cm^{-1}$: *transoid* $\mathbf{7}^{2+}$, $|D/hc| = 0.0029\ cm^{-1}$: doublet impurity; (*f*) simulation of the EPR spectrum shown above based on a 1.00 : 0.145 ratio of $\mathbf{8}^{2+}$, $|D/hc| = 0.0036\ cm^{-1}$: doublet impurity

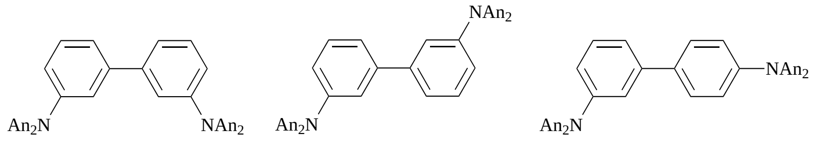

Planar geometries	**7**, *cisoid*	**7**, *transoid*	**8**
N to N distances	6.98 Å	8.43 Å	8.65 Å

Fig. 8 Hypothetical planar geometries for the diamines **7** and **8**

repulsion arising purely from this cause can be calculated as 25% greater for $\mathbf{7}^{2+}$ than $\mathbf{8}^{2+}$. Because the measured difference in the coulombic part of ΔE is much bigger than this (*ca.* 500%, Fig. 6) and is greater for $\mathbf{8}^{2+}$ than for $\mathbf{7}^{2+}$, most of it can be attributable to the fact that $\mathbf{8}^{2+}$, like the parent quinodimethane **2**, is coextensive in nature. The two centres are not wholly independent and there is 'leakage' of charge and spin between the two halves so that the charge and spin distributions substantially overlap. This produces a potential problem in the design of radical-ion based high-spin polymers.

Relevance to the design of high-spin polymers

Several groups are currently involved in the production of high-spin polymers in which the spin-bearing units are radical-cations and the spin is introduced by doping with an oxidising agent.[1,6,21] We have concentrated on doped polymers in which

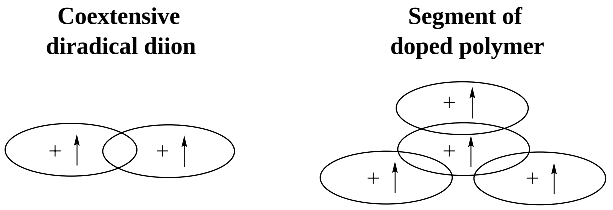

Fig. 9 Schematic representation of the charge and spin distributions in a coextensive diradical diion and of the local distributions in an equivalent polymer in which each radical ion site is linked to three nearest neighbour sites

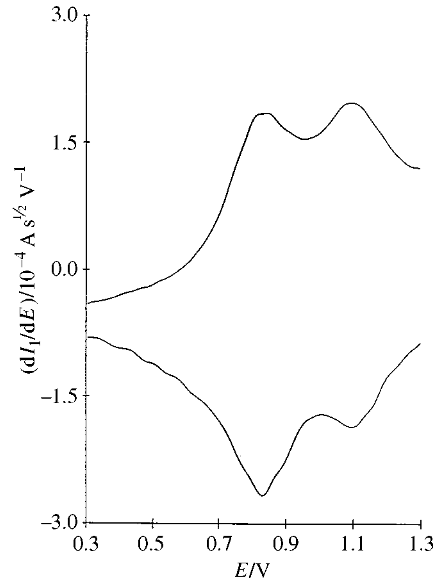

Fig. 10 Deconvolution cyclic voltammogram for the polymer **21** in dichloromethane (1.4 mg cm^{-3}) with 0.1 M tetrabutylammonium hexafluorophosphate as the supporting electrolyte

each spin-bearing centre is linked to three others in a randomly cross-linked network.[1] Application of percolation theory shows that > *ca.* 70% of the sites in such a polymer need to be doped before there is ferromagnetic coupling throughout the whole covalently linked framework. Depending on the molecular mass of the polymer, this should then give a material with either superparamagnetic or ferromagnetic properties. Unfortunately, both in our polymers and the corresponding linear polymers made by the group of Dougherty[21] (polymers in which each spin-bearing centre is linked to two others), the maximum doping levels that have been attained so far are < 35%: sufficient to demonstrate their high-spin character but well below the percolation limit. *A priori* it can be argued that these difficulties are the result of coulombic effects. As shown above, to ensure local ferromagnetic spin-coupling, the local topology of these polymers has to mimic that of a coextensive diradical diion.[1,2] There has to be spatial overlap of the unpaired spin distributions and hence (unfortunately) of the charges [Figs. 1(*a*), 2(*a*) and 9]. Furthermore, the stronger the ferromagnetic coupling, the bigger this overlap, the bigger the charge–charge repulsive effect and the more difficult the polymer will be to dope; a self-defeating and potentially fatal flaw in the whole strategy! This effect is rather different to that encountered in conventional doped polymers and it is difficult to predict how large it will be, particularly since we cannot estimate the extent to which charges will be shielded by ion-pairing. We have addressed the problem experimentally in two ways. First, as in this paper, we have studied the electrochemical behaviour of oligomers and secondly that of the polymers themselves. Most of the high-spin polymers we have made are based on a repeating *m*-phenylenediamine[22,23] or 3,4′-diaminobiphenyl[4,5] motif in which each centre is coextensively linked to three neighbouring centres as shown schematically in Fig. 9. The polymer **21**,[1] which is typical, was made from a Suzuki coupling reaction between the trisboronic acid **19** and the tribromide **20**. It is clearly structurally related to the dimer **8**. It is difficult to predict the extent of the hole–hole repulsion associated with the coextensive part of the charge distribution *a priori* since the local shielding effects, particularly those associated with ion-pairing, cannot be predicted. Hence, it should be possible to extrapolate a reasonable value for the extra hole–hole repulsion energy associated with the three nearest neighbour sites in the polymer **21** from the experimental results for the dimer **8**. Reference to Fig. 6 suggests that an upper limit will be 3 × (0.038–0.053 V) = 0.114–0.159 V based on upper limit estimates for the effective relative permittivity of the polymer, $\varepsilon_u = 5$–10. At a lower relative permittivity, because this is in the ‘ion-pairing regime’, the effect will be smaller (Fig. 4). The problem can also be addressed in a more direct manner through measurements on the polymers themselves.[23] Hence, for a solution of the polymer **21** in dichloromethane there are two *n*-electron oxidation steps at 0.29 and 0.55 V (with respect to ferrocene/ferrocenium ion under these conditions) and the width of each peak at half height is *ca.* 250 mV (Fig. 10). This polymer has two distinct types of site and the observed half-wave potentials are those expected for triarylamines of the type $\{C_6H_5[C_6H_3(OR)]\}_3N$ and Ph_3N, respectively.[15,24] The other arylamine polymers we have made[1] show similar or slightly smaller peak-broadening effects. The broadening apparent for the peaks arises in part from inhomogeneities frozen into the structure and unavoidable in a randomly cross-linked polymer, and in part from the coulombic factors. However, the above argument suggests that the latter contribution is <200 mV. Hence it seems that doping of these arylamine polymers is not coulombically limited. Particularly for the cross-linked polymers, a more likely explanation of the low doping levels achieved so far is the steric difficulty of incorporating counter-ions into a relatively rigid polymer network. This is unlikely to be an insuperable problem.

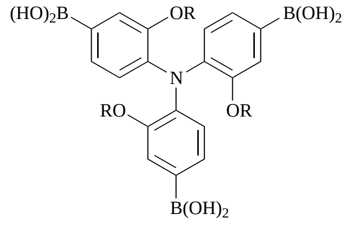

19, R = $C_{10}H_{21}$

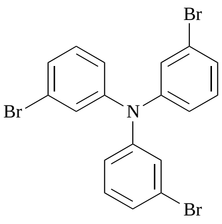

20

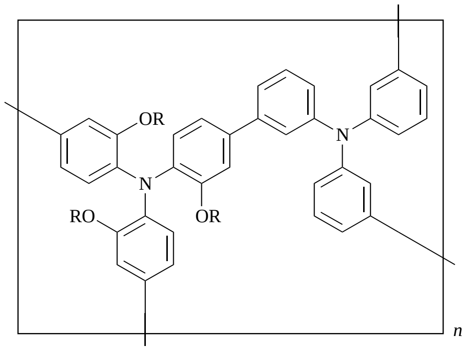

21, R = $C_{10}H_{21}$

Experimental

Melting points were determined on a Reichert Hot Stage and are uncorrected. Samples for combustion analysis were routinely dried by heating at 78 °C and 0.5 mmHg for 3 d. IR spectra were recorded on a Philips PU 9706 spectrophotometer. Only significant or assignable absorbances are reported. NMR spectra were recorded on a General Electric QE300, a Bruker

AC200 or a Bruker AM400 instrument. Chemical shifts are relative to tetramethylsilane; coupling constants are given in Hz. Mass spectra were obtained on a VG Autospec instrument. All peaks >20% of M^+ (and less intense peaks of particular significance) are reported. Solvents were routinely purified according to the procedures recommended by Perrin.[25] Column chromatography on silica refers to the use of Merck silica gel 9385 Type 60 and TLC to Whatman AL SIL G/UV plates.

3,3′-Dinitrobiphenyl 10†

3-Iodonitrobenzene (62.8 g, 0.25 mol) and copper powder (92.5 g, 1.44 g atom) were combined and suspended in dimethylformamide (DMF) (90 ml). The mixture was vigorously stirred and heated under reflux in an argon atmosphere. After 1.5 h, the reaction mixture was cooled to room temperature, extracted with hot chloroform (300 ml) and filtered hot to remove the inorganic residues. Upon cooling the product precipitated out as a creamy white solid. Recrystallisation from chloroform along with decolourising charcoal afforded **10** as colourless needles (14.7 g, 48%), mp 203–204 °C (lit.,[26] 201–202 °C) (Found: C, 58.9; H, 3.1%. $C_{12}H_8N_2O_4$ requires: C, 59.0; H, 3.3%); ν_{max}/cm^{-1} (Nujol) 3060 (C–H arom.), 1525 and 1345 (NO_2), 850 (C–N); δ_H(300 MHz, $CDCl_3$) 8.51 (2 H, s, 2 and 2′-H), 8.31 (2 H, d, *J* 8.1, 4 and 4′-H), 7.98 (2 H, d, *J* 7.8, 6 and 6′-H), 7.71 (2 H, t, *J* 7.9 and 8.1, 5 and 5′-H); *m*/*z*: 244 (M^+, 100%), 198 ($M^+ - NO_2$, 19%), 152 [$M^+ - (2 \times NO_2)$, 77%], 150 [$M^+ - (2 \times NO_2 - 2H)$, 48%].

3,3′-Diaminobiphenyl 11†

Tin powder (5.8 g, 49 mmol) was added gradually to a stirred suspension of **10** (2.65 g, 10.9 mmol) in concentrated hydrochloric acid (25 ml) and absolute ethanol (100 ml). The grey–blue suspension was heated under reflux for 1.5 h, poured onto an ice–water slurry, basified with 10% aqueous sodium hydroxide solution and extracted with diethyl ether (3 × 50 ml). The ethereal layer was washed with water, dried (Na_2SO_4) and concentrated *in vacuo*. Recrystallisation from ethanol gave the product (1.97 g, 98%) as an off-white solid, mp 82–83 °C (lit.,[26] 92–93 °C) (Found: C, 78.3; H, 6.7; N, 15.5%. $C_{12}H_{12}N_2$ requires: C, 78.3; H, 6.5; N, 15.2%); ν_{max}/cm^{-1} (Nujol) 3400, 3310 and 1630 (N–H), 1610 and 1585 (aromatic); δ_H(300 MHz, $CDCl_3$) 7.19 (2 H, t, *J* 7.8, 5 and 5′-H), 6.95 (2 H, d, *J* 7.5, 6 and 6′-H), 6.85 (2 H, s, 2 and 2′-H), 6.64 (2 H, d, *J* 7.8, 4 and 4′-H), 3.2 (4 H, s, $-NH_2$); *m*/*z*: 184 (M^+, 100%), 167 ($M^+ - NH_3$, 6%), 156 [$M^+ - (2 \times NH_2)$, 7%], 92 ($C_7H_8{}^+$, 9%).

N,*N*,*N*′,*N*′-Tetraanisyl-3,3′-diaminobiphenyl 7†

Compound **11** (1.47 g, 8 mmol), 4-iodoanisole (7.91 g, 33.8 mmol, 4.2 equiv.), copper powder (4.5 g, 71 mg atom) and potassium carbonate (19.6 g, 142 mmol) were combined in *o*-dichlorobenzene (30 ml) and heated under reflux with strong stirring for 18 h. The inorganic residues were filtered off, and these were washed with dichloromethane (100 ml). The organic phases were combined and concentrated under high vacuum. The crude product was subjected to column chromatography (40% hexane–dichloromethane) and then recrystallised from ethanol–benzene (1:1) to give an off-white crystalline solid (3.1 g, 64%), mp 206–207 °C (Found: C, 79.0; H, 6.1; N, 4.4%; M^+, 608.2666. $C_{40}H_{36}N_2O_4$ requires: C, 79.0; H, 5.9; N, 4.6%; M^+, 608.2675); ν_{max}/cm^{-1} (Nujol) 1595, 1510 and 1445 (aromatic), 1245 (C–O), 1040; δ_H(400 MHz, $CDCl_3$) 7.16 (2 H, t, *J* 7.9, 5 and 5′-H), 7.07 (2 + 8 H, d, *J* 8.9, anisyl protons *o*- to OMe and 2- and 2′-H), 6.96 (2 H, d, *J* 7.6, 6 and 6′-H), 6.82 (2 + 8 H, d, *J* 8.9, anisyl protons *o*- to nitrogens and 4- and 4′-H), 3.81 (12 H, s, OMe); δ_C(100 MHz, $CDCl_3$), 155.7, 149.0, 142.1, 140.0, 129.0, 126.4, 119.5, 119.3, 114.6, 55.5; *m*/*z*: 608 (M^+, 100%), 593 ($M^+ - Me$, 8%), 304 (0.5 M^-, 26%), 289 (0.5$M^+ -$ Me, 20%).

N,*N*-Dianisyl-3-nitroaniline 13

3-Nitroaniline (1.38 g, 10 mmol), 4-iodoanisole (5.85 g, 25 mmol), copper powder (5.12 g, 80 mg atom) and potassium carbonate (10.7 g, 78 mmol) were combined in DMF (25 ml) and heated under reflux with strong mechanical stirring under argon for 12 h. The inorganic residues were filtered off and the remaining material was taken up in chloroform (500 ml), washed with distilled water (5 × 50 ml), dried (Na_2SO_4) and concentrated *in vacuo*. The final traces of DMF were removed under high vacuum. Column chromatography on flash silica (hexane–chloroform, 1:1) gave the product (1.83 g, 52%) as a yellow solid (mp 117–118 °C) (Found: C, 68.4; H, 5.2; N, 8.0%; M^+, 350.1277. $C_{20}H_{18}N_2O_4$ requires: C, 68.6; H, 5.1; N, 8.0%; M^+, 350.1267); ν_{max}/cm^{-1} (Nujol) 1600, 1510 and 1460 (aromatic), 1590 and 1330 (NO_2), 1230 (C–O), 820 (C–N); δ_H(300 MHz, $CDCl_3$) 7.66 (1 H, s, *o*- to NO_2 and NAn_2), 7.60 (1 H, d, *J* 8.1, *o*- to NO_2 and *p*- to NAn_2), 7.24 (1 H, t, *J* 7.8 and 8.1, *m*- to NO_2 and NAn_2), 7.09 (5 H, d, *J* 8.8, 4 anisyl protons *o*- to OMe and 1 H *o*- to NAn_2 and *p*- to NO_2), 6.88 (4 H, d, *J* 8.9, anisyl protons *m*- to OMe), 3.81 (6 H, s, OMe); δ_C(50 MHz, $CDCl_3$) 156.9, 150.1, 149.2, 139.4, 129.4, 127.3, 124.1, 115.1, 113.1, 112.8, 55.5; *m*/*z*: 350 (M^+, 100%), 335 ($M^+ - Me$, 60%), 320 [$M^+ - (2Me)$, 17%], 289 [$M^+ - (Me$ and $NO_2)$, 19%], 230 (46%).

N,*N*-Dianisyl-3-aminoaniline 14

Raney nickel (4 ml, *ca.* 2.4 g, 40 mg atom) was added to a red solution of *N*,*N*-dianisyl-3-nitroaniline (3.08 g, 8.8 mmol) in ethanol (120 ml) and the mixture was stirred under an atmosphere of hydrogen at room temperature for 18 h. The nickel catalyst was removed by filtration through celite at the pump and the ethanol removed *in vacuo* to give a quantitative yield of the amine (2.82 g, 100%) as an air-sensitive off-white solid (mp 89–90 °C) (Found: M^+, 320.1523. $C_{20}H_{20}N_2O_2$ requires 320.1525); ν_{max}/cm^{-1} (Nujol) 3480 (br) and 1605 (N–H), 1575 and 1490 (aromatic), 1230 (C–O); δ_H(300 MHz, $CDCl_3$) 7.02 (4 H, d, *J* 8.9, anisyl protons *o*- to OMe), 6.91 (1 H, t, *J* 7.9, *m*- to NH_2 and to NAn_2), 6.77 (4 H, d, *J* 8.9, anisyl protons *m*- to OMe), 6.30 (1 H, d, *J* 7.9, *o*- to NAn_2 and *p*- to NH_2), 6.22 (1 H, s, *o*- to NAn_2 and NH_2), 6.16 (1 H, d, *J* 7.9, *o*- to NH_2 and *p*- to NAn_2), 3.78 (6 H, s, OMe), 3.41 (2 H, br s, $-NH_2$); δ_C(50 MHz, $CDCl_3$) 155.6, 150.2, 147.0, 141.1, 129.7, 126.6, 114.5, 111.5, 107.8, 107.5, 55.5; *m*/*z*: 320 (M^+, 100%), 305 ($M^+ - Me$, 55%), 97 (27%).

N,*N*-Dianisyl-3-bromoaniline 15

Compound **14** (2.82 g, 8.8 mmol) was suspended as a salt in hydrobromic acid (48%, 50 ml), cooled to <0 °C and treated with a cold solution of sodium nitrite (620 mg, 8.98 mmol) in distilled water (15 ml), which was added over 1 h. The mixture was stirred at 0 °C for 15 min further, added to a cooled solution of copper(I) bromide (4.58 g, 67 mmol) in hydrobromic acid (30 ml), stirred for 1 h at 0 °C, and gradually warmed to room temperature before being heated to *ca.* 90 °C to release all the nitrogen from the diazonium salt. The crude reaction product was diluted in water (50 ml), extracted with chloroform (2 × 150 ml), washed with dilute aqueous sodium hydroxide solution (2 M), then brine and then with water, before being dried ($MgSO_4$). The crude material was purified by column chromatography on flash silica (eluting with hexane–chloroform, 3:1 v/v) and then by recrystallisation (ethanol–water) which gave the pure product as a white powder (1.62 g, 48%), mp 78–81 °C (Found: M^+, 383.0514. $C_{20}H_{17}N^{79}BrO_2$ requires 383.0521); ν_{max}/cm^{-1} (Nujol) 1590, 1505 and 1440 (aromatic), 1245 (C–O), 1030; δ_H(300 MHz, $CDCl_3$) 7.31 (1 H, d, *J* 8.8, *p*- to NAn_2 and *o*- to Br), 7.11 (1 H, d, *J* 2.6, *o*- to Br

---

† Although, in general, 3-nitro and 3-amino biphenyls are much less carcinogenic than their 4-nitro and 4-amino counterparts[7] they still need to be treated as potential carcinogens and with CAUTION.

and NAn_2), 7.04 (4 H, d, *J* 8.8, anisyl-H *o-* to OMe), 6.84 (5 H, d, *J* 8.8, 4 anisyl-H *m-* to OMe and 1 H *m-* to Br and NAn_2), 6.68 (1 H, dd, *J* 8.8 and 2.6, *p-* to Br and *o-* to NAn_2), 3.80 (6 H, s, OMe); *m*/*z*: 385 [$M^+(^{81}Br)$, 100%], 383 [$M^+(^{79}Br)$, 99%], 370 [$M^+(^{81}Br) - Me$, 73%], 368 [$M^+(^{79}Br) - Me$, 72%], 305 ($M^+ - Br$, 7%), 290 (305 − Me, 6%).

N,N-Dianisylaniline 16

Freshly distilled aniline (5.53 g, 59 mmol), 4-iodoanisole (28 g, 119.6 mmol, 2.02 equiv.), copper(I) iodide (35 g, 184 mmol) and potassium carbonate (27 g, 196 mmol) were mixed in *o*-dichlorobenzene (100 ml) and heated under reflux for 66 h with vigorous mechanical stirring. After filtering off the inorganics, the crude was taken up in chloroform (200 ml) and concentrated *in vacuo*. The crude product was initially passed through a short column of silica and then further purified by chromatography on silica (eluting with hexane–dichloromethane, 2:1) to give **16** as pale-yellow needles (14.9 g, 83%), mp 103–104 °C (lit.,[27] 103 °C) (Found: C, 78.5; H, 6.5; N, 4.3%; M^+, 305.1412. $C_{20}H_{19}NO_2$ requires: C, 78.7; H, 6.2; N, 4.6%; M^+, 305.1416); ν_{max}/cm^{-1} (Nujol) 1595, 1510 and 1445 (aromatic), 1250 (C–O); δ_H(300 MHz, $CDCl_3$) 7.16 (2 H, t, *J* 7.5, phenyl protons *m-* to NAn_2), 7.04 (4 H, d, *J* 8.9, anisyl protons *o-* to OMe), 6.93 (2 H, d, *J* 7.9, phenyl protons *o-* to NAn_2), 6.82 (1 H, m, phenyl proton *p-* to NAn_2), 6.80 (4 H, d, *J* 8.9, anisyl *m-* to OMe), 3.79 (6 H, s, –OMe); δ_C(50 MHz, $CDCl_3$) 155.7, 148.7, 141.1, 128.9, 126.3, 120.9, 120.5, 114.6, 55.5; *m*/*z*: 305 (M^+, 100%), 290 ($M^+ - Me$, 79%), 77 ($C_6H_5{}^+$, 20%).

N,N-Dianisyl-4-bromoaniline 17

Bromine (870 mg, 5.4 mmol) in chloroform (15 ml) was added dropwise to a stirred solution of **16** (1.61 g, 5.4 mmol) in chloroform (50 ml) at 0 °C. After stirring overnight, the crude product was added to water (30 ml), extracted further with chloroform, dried ($MgSO_4$), subjected to column chromatography on silica (eluting with hexane–chloroform, 1:1) and recrystallised from ethanol to give a white crystalline solid (1.92 g, 95%), mp 91–92 °C (Found: C, 62.7; H, 4.4; N, 3.6; Br, 20.8%; M^+, 385.0496. $C_{20}H_{18}{}^{81}BrNO_2$ requires: C, 62.5; H, 4.7; N, 3.7; Br, 20.8%; M^+, 385.0500); ν_{max}/cm^{-1} (Nujol) 1592, 1510 and 1495 (aromatic), 1250 (C–O); δ_H(300 MHz, C_6D_6), 7.17 (2 H, d, *J* 8.8, *o-* to Br), 6.95 (4 H, d, *J* 8.9, *o-* to OMe), 6.75 (2 H, d, *J* 8.8, *m-* to Br), 6.68 (4 H, d, *J* 8.9, *m-* to OMe), 3.27 (6 H, s, OMe); δ_C(50 MHz, $CDCl_3$) 156.0, 147.2, 140.5, 131.8, 126.6, 121.9, 114.8, 115.6, 55.5; *m*/*z*: 385 [$M^+(^{81}Br)$, 100%], 383 [$M^+(^{79}Br)$, 99%], 370 [$M^+(^{81}Br) - Me$, 66%], 368 [$M^+(^{79}Br) - Me$, 66%], 305 ($M^+ - Br$, 37%), 290 ($M^+ - Br - Me$, 31%).

N,N-Dianisyl-4-(1,3,2-dioxaborolan-2-yl)aniline 18

Compound **17** (161 mg, 418 µmol) in dry tetrahydrofuran (THF) (3 ml) was cooled to −78 °C and butyllithium (1.6 M in hexanes, 0.3 ml, 480 µmol, 1.15 equiv.) was added dropwise under argon. A purple solution resulted which was allowed to reach room temperature gradually and was stirred at this temperature for 1 h before being cooled to −78 °C. The lithiated material was cannulated into a solution of triisopropyl borate (350 mg, 1.86 mmol, 3.9 equiv.), in dry THF (4 ml) also held at −78 °C under argon, and was slowly warmed to ambient temperature. After stirring for 5.5 h the cloudy mixture was hydrolysed with 2 M HCl (2.5 ml) affording a turquoise solution. Distilled water (6 ml) was added and the organic layer separated by extraction with diethyl ether (10 ml), combined with further ethereal extracts of the aqueous layer and concentrated *in vacuo*. The crude boronic acid was purified by dissolving in 2 M aqueous sodium hydroxide solution (2 ml), washing with chloroform, reprecipitating with concentrated hydrochloric acid, and collecting by filtration at the pump. Dichloromethane (10 ml) and ethane-1,2-diol (150 mg, 2.2 mmol) were added and the solvent removed at normal pressure to remove traces of water azeotropically. The mixture was subsequently heated at 100 °C and 0.1 mmHg, then washed with water to give the cyclic ester (102 mg, 65%) (Found: M^+, 375.1649. $C_{22}H_{22}N^{11}BO_4$ requires 375.1642); ν_{max}/cm^{-1} (Nujol) 1600 (aromatic), 1380 and 1340 (B–O), 1250 (C–O); δ_H(200 MHz, $CDCl_3$), 7.59 (2 H, d, *J* 8.7, *o-* to boron), 7.08 (4 H, d, *J* 9.0, *o-* to OMe), 6.86 (2 H, d, *J* 8.7, *m-* to boron), 6.84 (4 H, d, *J* 9.1, *m-* to OMe), 4.33 (4 H, s, CH_2CH_2), 3.80 (6 H, s, OMe); *m*/*z*: 375 (M^+, 39%), 360 ($M^+ - Me$, 18%), 305 ($M^+ - BO_2C_2H_4$, 100%), 290 (305 − Me, 71%).

N,N,N′N′-Tetraanisyl-3,4′-diaminobiphenyl 8

Compound **18** (676 mg, 1.8 mmol), compound **15** (749 mg, 1.95 mmol, 1.08 equiv.), $Pd(PPh_3)_4$ (40 mg, 2 mol%) and barium hydroxide (1.2 g) were combined in toluene (40 ml) and degassed with argon and the mixture was heated under reflux overnight with strong magnetic stirring. Distilled water was added and the layers were separated; the organic phase washed further with distilled water (10 ml), 2 M aqueous sodium hydroxide solution (5 ml), then water (10 ml), dried (Na_2SO_4), and concentrated *in vacuo*. The crude product was chromatographed on silica (40% hexane in dichloromethane) to give the product as a light-brown solid (818 mg, 75%), mp 199–202 °C (Found: C, 79.2; H, 5.8; N, 4.5%; M^+, 608.2701. $C_{40}H_{36}N_2O_4$ requires: C, 79.0; H, 5.9; N, 4.6%; M^+, 608.2675); ν_{max}/cm^{-1} (Nujol) 1590, 1565, 1500 (aromatic), 1250 (C–O); δ_H(400 MHz, $CDCl_3$) 7.29 (2 H, d, *J* 8.7, 2′-H), 7.20 (1 H, t, *J* 7.8, 5-H), 7.14 (1 H, s, 2-H), 7.07 (1 + 4 H, d, *J* 8.9, anisyl *o-* to OMe and 6-H), 6.92 (2 H, d, *J* 8.6, 3′-H), 6.83 (9 H, d, *J* 8.9, anisyl *m-* to OMe and 4-H), 3.80 (12 H, s, OMe); δ_C(100 MHz, $CDCl_3$) 155.8, 155.6, 149.1, 148.0, 141.6, 141.1, 140.8, 133.1, 129.1, 127.4, 126.5, 126.4, 120.6, 119.1, 119.0, 118.9, 114.64, 114.61, 55.5; *m*/*z*: 608 (M^+, 100%), 593 ($M^+ - Me$, 10%), 502 [$M^+ -$ (PhOMe) + H, 25%], 304 (0.5 M^+, 31%), 289 (304 − Me, 15%).

Studies by cyclic voltammetry

These studies were carried out using a conventional three-electrode system coupled to an EG & G Model 362 scanning potentiostat with the system controlled by an Amstrad PC 1640 personal computer running the CONDECON310 cyclic voltammetry software. The working electrode was a small platinum disc, the counter electrode a 1 cm^2 platinum sheet and the reference electrode a silver wire immersed in a saturated lithium chloride–chloroform mixture containing 0.1 M tetrabutylammonium hexafluorophosphate as the supporting electrolyte. The benzonitrile used as the solvent was freshly purified by the procedures described in Perrin,[25] passed through a short column of silica and used immediately. The substrates **7** and **8** were freshly chromatographically purified before use. The supporting electrolyte was tetrabutylammonium hexafluorophosphate. The solutions were purged with argon prior to the start of data acquisition. Ferrocene was used as the standard and its oxidation potential checked before each new experiment for the particular solvent or solvent mixture being used. For the voltammograms shown in Fig. 3 the potential was swept in the anodic direction (upper trace) and the lower trace represents the reverse sweep in the cathodic direction.

Studies of the oxidations by EPR spectroscopy

These studies were carried out using very similar apparatus. EPR spectra were recorded on either a Varian E-6 spectrometer or a Bruker ER 200 spectrometer (with a Bruker ESP 1600 data acquisition system), both fitted with Bruker 4111 VT variable temperature units.

Acknowledgements

We thank the EPSRC for the award of a Research Studentship to D. R. M. and of a Post-Doctoral Fellowship to K. M. N., and Dr R. Luo for assistance and advice in the cyclic voltammetry studies.

References

1 R. J. Bushby, D. R. McGill and K. M. Ng, in *Magnetism; A Supramolecular Function*, ed. O. Kahn, Kluwer, Dordrecht, 1996, pp. 181–204.

2 D. A. Dougherty, *Acc. Chem. Res.*, 1991, **24**, 88; W. T. Borden and E. R. Davidson, *J. Am. Chem. Soc.*, 1977, **99**, 4587.

3 G. Allison, R. J. Bushby and J.-L. Paillaud, *J. Mater. Sci., Mater. Electronics*, 1994, 67.

4 Y. Teki, I. Fujita, T. Takui, T. Kinoshita and K. Itoh, *J. Am. Chem. Soc.*, 1994, **116**, 11 499.

5 M. Minato, P. M. Lathi and H. van Willigen, *J. Am. Chem. Soc.*, 1993, **115**, 4532.

6 R. J. Bushby and K. M. Ng, *Chem. Commun.*, 1996, 659; K. Yoshizawa, K. Tanaka, T. Yamabe and J. Yamauchi, *J. Chem. Phys.*, 1992, **96**, 5516; A. Ito, K. Ota, K. Tanaka, T. Yamabe and K. Yoshizawa, *Macromolecules*, 1995, **28**, 5618.

7 M. Nohara, T. Hirayama, Y. Fujioka, S. Ozasa, E. Ibuki and S. Fukui, *Mutation Res.*, 1985, **149**, 9.

8 J. Lindley, *Tetrahedron*, 1984, **40**, 1433, and references therein.

9 Y. Hoshino, N. Miyaura and A. Suzuki, *Bull. Chem. Soc. Jpn.*, 1988, **61**, 3008.

10 I. G. C. Coutts, H. R. Goldschmid and O. C. Musgrave, *J. Chem. Soc.* (*C*), 1970, 488.

11 K. B. Oldham and J. Spanier, *J. Electroanal. Chem.*, 1970, **26**, 331; K. B. Oldham, *Anal. Chem.*, 1972, **44**, 196; M. Grenness and K. B. Oldham, *Anal. Chem.*, 1972, **44,** 1121.

12 R. J. Bushby and G. J. Ferber, *J. Chem. Soc., Perkin Trans. 2*, 1976, 1695; R. J. Bushby and H. L. Steel, *J. Chem. Soc., Perkin Trans. 2*, 1990, 1143.

13 N. Taylor, T. Boddington, I. Dobson, B. Gill, R. Luo and B. Shaw, in *Molecular Electrochemistry of Inorganic, Bioorganic and Organometallic compounds*, ed. A. J. L. Pombeiro and J. A. McCleverty, Kluwer, Dordrecht, 1993, p. 467; A. Blagg, S. W. Carr, G. R. Cooper, I. D. Dobson, J. B. Gill, D. C. Goodall, B. L. Shaw, N. Taylor and T. Boddington, *J. Chem. Soc., Dalton Trans.*, 1985, 1213.

14 I. D. Dobson, Ph.D. Thesis, University of Leeds, 1986.

15 E. T. Seo, R. F. Nelson, J. M. Fritsch, L. S. Marcoux, D. W. Leedy and R. N. Adams, *J. Am. Chem. Soc.*, 1966, **88**, 3498.

16 R. J. Bushby and K. M. Ng, *J. Chem. Soc., Perkin Trans. 2*, 1996, 1053.

17 M. Brown, G. R. Freeman and R. I. Walter, *J. Am. Chem. Soc.*, 1977, **99**, 6910; K. S. Hayes, M. Nagamo, J. F. Blount and K. Mislow, *J. Am. Chem. Soc.*, 1980, **102**, 2773; L. A. Chetkina, E. G. Popova, V. M. Vozzhennikov and B. V. Kotov, *Zh. Strukt. Khim.*, 1976, **17**, 114; E. G. Popova, L. A. Chetkina and B. V. Kotov, *Zh. Strukt. Khim.*, 1976, **17**, 510; J. L. Fox, C. H. Chen and H. R. Luss, *J. Org. Chem.*, 1987, **52**, 2980; P. S. Engel, A. K. M. M. Hogue, J. N. Scholz, H. J. Shine and K. H. Whitmire, *J. Am. Chem. Soc.*, 1988, **110**, 7880; E. Chiba, *Acta Crystallogr., Sect. C*, 1993, **49**, 1511; E. Muller and H.-B. Burgi, *Acta Crystallogr., Sect. C*, 1989, **45**, 1400; G. V. Gridunova, V. E. Shiklover, Yu. T. Struchkov, I. G. Il'ina, O. V. Mikhalev and V. I. Potapov, *Kristallografiya*, 1989, **34**, 87; S. L. Reynolds and R. P. Scaringe, *Cryst. Struct. Commun.*, 1982, **11**, 1129; C. Okumura, Y. T. Osano, T. Murayama and T. Matsuzaki, *Anal. Sci.*, 1990, **6**, 485; H. Inada, K. Obnishi, S. Nomura, A. Higuchi, H. Nakano and Y. Shirota, *J. Mater. Chem.*, 1994, **4**, 171; S. J. Stoudt, P. Gopolan, B. Kahr and J. E. Jackson, *Struct. Chem.*, 1994, **5**, 335; A. N. Sobdev, V. K. Belsky, N. Yu. Chernikova and E. N. Guryanova, *Acta Crystallogr., Sect. C*, 1985, **41**, 967.

18 E. Wasserman, L. C. Snyder and W. A. Yager, *J. Chem. Phys.*, 1964, **41**, 1763.

19 S. S. Eaton, K. M. More, B. M. Sawant and G. R. Eaton, *J. Am. Chem. Soc.*, 1983, **105**, 6560.

20 G. Allinson, R. J. Bushby, J.-L. Paillaud, D. Oduwole and K. Sales, *J. Am. Chem. Soc.*, 1993, **115**, 2062.

21 M. M. Murray, P. Kaszynski, D. A. Kaisaki, W. Chang and D. A. Dougherty, *J. Am. Chem. Soc.*, 1994, **116**, 8152.

22 K. Yoshizawa, A. Chano, A. Ito, K. Tanaka, T. Yamabe, H. Fujita, J. Yamauchi and M. Shiro, *J. Am. Chem. Soc.*, 1992, **114**, 5994; K. R. Stickley and S. C. Blackstock, *J. Am. Chem. Soc.*, 1994, **116**, 11 576; P. M. Lathi, C. Ling, N. Yoshioka, F. C. Rossitto and H. van Willigen, *Mol. Cryst. Liq. Cryst.*, 1993, **233**, 17.

23 M. M. Wienk and R. A. J. Janssen, *Chem. Commun.*, 1996, 267.

24 R. J. Bushby, D. R. McGill and N. Taylor, unpublished results.

25 *Purification of Laboratory Chemicals*, D. D. Perrin, W. L. F. Armarego and D. R. Perrin, 2nd edn., Pergamon Press, Oxford, 1980.

26 H. A. Staab and F. Binnig, *Chem. Ber.*, 1967, **100**, 293.

27 W. Lamm, W. Jugelt and F. Pragst, *J. Prakt. Chem.*, 1975, **317**, 284.

Paper 6/05722E
Received 16*th August* 1996
Accepted 6*th March* 1997